

FIRST RESULTS FROM THE SUBMILLIMETER POLARIMETER FOR ANTARCTIC REMOTE OBSERVATIONS: EVIDENCE OF LARGE-SCALE TOROIDAL MAGNETIC FIELDS IN THE GALACTIC CENTER

G. NOVAK,¹ D. T. CHUSS,¹ T. RENBARGER,¹ G. S. GRIFFIN,² M. G. NEWCOMB,² J. B. PETERSON,²
R. F. LOEWENSTEIN,³ D. PERNIC,³ AND J. L. DOTSON⁴

Received 2001 September 5; accepted 2002 December 23; published 2003 January 15

ABSTRACT

We have observed the linear polarization of 450 μm continuum emission from the Galactic center, using a new polarimetric detector system that is operated on a 2 m telescope at the South Pole. The resulting polarization map extends ~ 170 pc along the Galactic plane and ~ 30 pc in Galactic latitude, and thus covers a significant fraction of the central molecular zone. Our map shows that this region is permeated by large-scale toroidal magnetic fields. We consider our results together with radio observations that show evidence of poloidal fields in the Galactic center and with Faraday rotation observations. We compare all of these observations with the predictions of a magnetodynamic model for the Galactic center that was proposed in order to explain the Galactic Center Radio Lobe as a magnetically driven gas outflow. We conclude that the observations are fundamentally consistent with the model.

Subject headings: Galaxy: center — ISM: magnetic fields — polarization

1. INTRODUCTION

Beginning with the discovery of the first examples of Galactic center nonthermal filaments (Yusef-Zadeh, Morris, & Chance 1984), radio observers have garnered a steadily growing body of observational evidence pointing toward the existence of large-scale, ordered magnetic fields in the Galactic center region, with an overall orientation that is perpendicular to the Galactic plane (Morris 1998). The main tracers of the magnetic field are the Galactic center nonthermal filaments themselves. Such filaments have now been found at a variety of locations throughout the central few hundred parsecs (LaRosa et al. 2000). They are generally orthogonal to the Galactic plane, and radio polarimetry has confirmed that the magnetic fields in these synchrotron-emitting structures run longitudinally (Lang, Morris, & Echevarria 1999). A more diffuse component of nonthermal emission is also present, but due to Faraday rotation/depolarization, polarimetry of this diffuse component does not always reliably determine the projected field direction. For the few cases in which it does, the field turns out again to be perpendicular to the Galactic plane (Tsuboi et al. 1986). This accumulation of radio observations has led to the hypothesis that most of the volume of the Galactic center is permeated by a large-scale magnetic field that is poloidal or perhaps axial. Here we are using a cylindrical coordinate system for the Galaxy, and poloidal and axial refer, respectively, to the component in the r - z plane and the component along z .

Along with this relativistic ionized gas, the Galactic center contains a concentration of dense molecular gas, extending ~ 450 pc along the Galactic plane and ~ 50 pc in Galactic latitude (Oka et al. 1998). It is possible to map the magnetic field in this “central molecular zone” by observing the polarization of far-infrared/submillimeter thermal emission from magnetically aligned dust grains. The measured direction of the E -

vector will be orthogonal to the direction of the magnetic field, as projected onto the plane of the sky (Lazarian 2000 and references therein). Several flux peaks within the central molecular zone have been studied using this polarimetry technique, but no strong evidence of poloidal or axial fields has been found. In fact, although the projected magnetic field directions vary over a very wide range, they tend to be more nearly parallel to the Galactic plane than perpendicular to it (Novak et al. 2000 and references therein). For this reason, Novak et al. (2000) suggested that the molecular gas in the Galactic center is permeated by a toroidal field (see also Morris et al. 1992).

In this Letter, we present a new submillimeter polarimetric map of the Galactic center that has more sky coverage than all previous far-infrared/submillimeter polarimetric maps of this region combined. Our polarization map has an extent of ~ 170 pc along the Galactic plane and ~ 30 pc in Galactic latitude, and thus covers a significant fraction of the central molecular zone. The observations were carried out at South Pole station, using the 2 m Viper telescope and a new submillimeter polarimeter called SPARO (Submillimeter Polarimeter for Antarctic Remote Observations). The data presented here are the first scientific results obtained with the SPARO instrument.

2. OBSERVATIONS AND RESULTS

Viper is an off-axis submillimeter telescope of ~ 2 m diameter, located at Amundsen-Scott South Pole station (Peterson et al. 2000). During the observations described here, the SPARO instrument was installed at Viper’s focal plane. SPARO is a 9 pixel submillimeter array polarimeter incorporating ^3He -cooled detectors (T. Renbarger et al. 2003, in preparation; Dotson et al. 1998). Because the South Pole is an exceptionally good submillimeter site (Lane 1998), SPARO obtains extremely good sensitivity to spatially extended, low surface brightness emission. The observations were carried out during 2000 April–July.

SPARO’s spectral passband is centered at $\lambda_0 = 450 \mu\text{m}$, with a fractional bandwidth $\Delta\lambda/\lambda_0 = 0.10$. The instrument observes simultaneously at nine sky positions, with the pixels arranged in a 3×3 square pattern. The pixel-to-pixel separation is $3'.5$, and the beam FWHM was determined to be

¹ Department of Physics and Astronomy, Northwestern University, 2145 Sheridan Road, Evanston, IL 60208-2900; g-novak@northwestern.edu.

² Department of Physics, Carnegie Mellon University, 7325 Wean Hall, 5000 Forbes Avenue, Pittsburgh, PA 15213-3890.

³ Yerkes Observatory, University of Chicago, 373 West Geneva Street, Williams Bay, WI 53191.

⁴ NASA Ames Research Center, MS 245-6, Moffett Field, CA 94035.

TABLE 1
POLARIZATION RESULTS

$\Delta\alpha^a$ (arcmin)	$\Delta\delta^a$ (arcmin)	P (%)	σ_p	ϕ^b	σ_ϕ
26.7	43.7	1.47	0.53	125.0	10.0
21.8	41.3	0.74	0.17	19.7	7.5
28.2	38.7	0.68	0.15	89.8	6.3
31.5	37.4	1.10	0.34	93.2	8.9
26.9	35.4	0.96	0.13	78.3	3.4
30.1	34.1	1.00	0.33	76.4	8.6
22.3	33.5	0.67	0.14	95.8	6.5
14.9	32.7	1.35	0.43	112.9	9.0
25.6	32.2	0.93	0.17	75.6	4.8
18.0	31.5	1.20	0.33	114.5	8.2
21.2	30.2	1.71	0.34	110.7	6.0
20.1	26.8	1.99	0.60	99.1	8.4
15.5	24.9	2.55	0.60	100.5	6.6
13.9	20.5	2.25	0.76	124.0	9.5
8.5	17.0	2.13	0.54	121.7	7.2
8.0	15.3	1.74	0.48	116.9	7.7
3.8	14.0	1.42	0.25	103.8	4.8
7.3	12.8	1.08	0.22	119.7	5.8
10.5	11.5	1.53	0.34	126.3	6.3
2.7	10.9	1.34	0.26	114.6	5.4
6.0	9.6	1.02	0.22	112.7	6.4
-5.2	5.9	2.13	0.74	108.2	9.5
-1.5	4.8	0.98	0.25	116.7	7.3
1.8	3.5	0.73	0.18	87.6	7.2
0.5	0.2	0.81	0.18	102.5	6.5
3.7	-1.1	1.09	0.22	103.1	5.9
1.6	-1.4	2.22	0.49	105.4	6.3
-4.5	-1.9	1.99	0.60	117.4	8.4
-0.8	-3.0	1.56	0.17	118.9	3.1
2.4	-4.3	1.57	0.21	110.6	3.8
-7.1	-4.6	1.31	0.45	120.1	9.6
-3.8	-5.9	0.83	0.27	117.9	9.2
-0.6	-7.2	1.53	0.27	120.8	5.1
-8.4	-7.8	1.57	0.43	155.9	7.9
-1.9	-10.5	2.00	0.31	116.2	4.5
-6.4	-12.4	2.31	0.40	122.8	4.9
-3.2	-13.7	1.48	0.36	119.5	6.7

^a Offsets in right ascension and declination are measured relative to the position of Sgr A*.

^b Angle of the E -vector of the polarized radiation, measured in degrees from north-south, increasing counterclockwise.

$5' \pm 1'$. The pointing accuracy was $\pm 1'$. We used two sky reference positions, separated from the main observing position by $+0.5$ and -0.5 in cross-elevation, respectively.

The instrumental polarization was determined by calibrating on the Moon and on the intensity peak of Sgr B2. The Moon was assumed to be unpolarized near its center, and the magnitude and direction of polarization for Sgr B2 were assumed to be given by $P = 0.49\%$ and $\phi = 82^\circ$, respectively. These values for Sgr B2 were obtained by averaging the $350 \mu\text{m}$ polarimetry results of Dowell et al. (1998) over the area of SPARO's beam. For the purposes of this calibration, we have ignored the wavelength dependence of the polarization. However, this effect should be small (Vaillancourt 2002; Dowell et al. 1998). Instrumental polarization values obtained for a given pixel using the two independent calibrators typically agreed to within $\sim 0.2\%$. Based on these calibrations and on other tests (T. Renbarger et al. 2003, in preparation), we are confident that the level of systematic error in our measurements is less than 0.3% . This translates into an uncertainty in the polarization angle of less than $(9^\circ)(1.0\%/P)$.

In Table 1, we present our polarization results with associated statistical errors (σ_p and σ_ϕ) for sky positions where we obtained polarization detections of statistical significance, $P/\sigma_p > 2.75$. Figure 1 shows these results using bar symbols. The orientation of each bar gives the inferred magnetic field direction, which

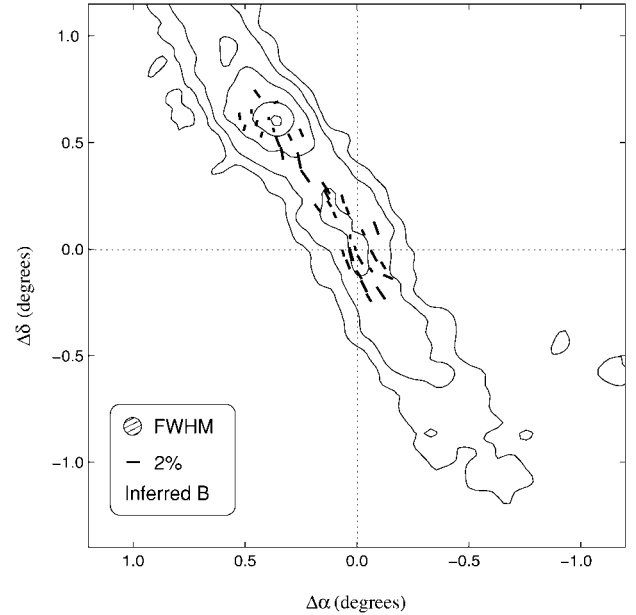


FIG. 1.—Results of $450 \mu\text{m}$ polarimetry (bars) and photometry (contours) of the Galactic center, obtained using SPARO. The distribution of $450 \mu\text{m}$ flux closely follows the Galactic plane, which lies at a position angle of $+31^\circ$. Coordinate offsets are measured with respect to the location of Sgr A*. Each bar is drawn parallel to the inferred magnetic field direction (i.e., perpendicular to the E -vector of the measured submillimeter polarization), and the length of the bar indicates the measured degree of polarization (see key at bottom left). Contours are drawn at 0.075, 0.15, 0.30, 0.60, and 0.95 times the peak flux, which is located at the position of Sgr B2. For clarity, negative contours are not shown. The reference beam offsets were the same for polarimetry and photometry and are given in § 2. The $5'$ beam of SPARO is shown in the key. Positive Galactic latitudes lie toward the upper right of the figure, and positive Galactic longitudes lie toward the upper left.

is orthogonal to the E -vector of the measured polarization, and the length of the bar is proportional to the degree of polarization. The bars are superposed on a photometric map that was also obtained using SPARO. Clearly visible in the photometric map is the large concentration of molecular gas that is associated with the innermost few hundred parsecs of the Galaxy. (One degree corresponds to 140 pc for an assumed distance of 8.0 kpc.) This concentration of gas is asymmetric, with the highest column density at the position of Sgr B2 displaced toward positive Galactic longitudes from the location of Sgr A*. Our results imply that the magnetic field permeating the Galactic center molecular gas, when projected onto the plane of the sky, is for the most part parallel to the Galactic plane.

3. DISCUSSION

The simplest explanation for this alignment of projected field direction with Galactic plane is that the molecular gas in the Galactic center is threaded by a large-scale magnetic field having a toroidal (i.e., azimuthal) configuration. As we discussed in § 1, previous far-infrared/submillimeter polarimetry had already suggested such a toroidal field. However, the SPARO map covers much more sky area. Furthermore, in the SPARO map, the observed magnetic field “vectors” are much more tightly aligned with the Galactic plane than was the case for any earlier map. The SPARO results thus provide new and stronger evidence of the existence of this toroidal large-scale field.

Figure 2 contrasts SPARO results with nonthermal filaments (gray scale) representing evidence of poloidal, or perhaps axial, magnetic fields. Hereafter, in discussing the field traced by the

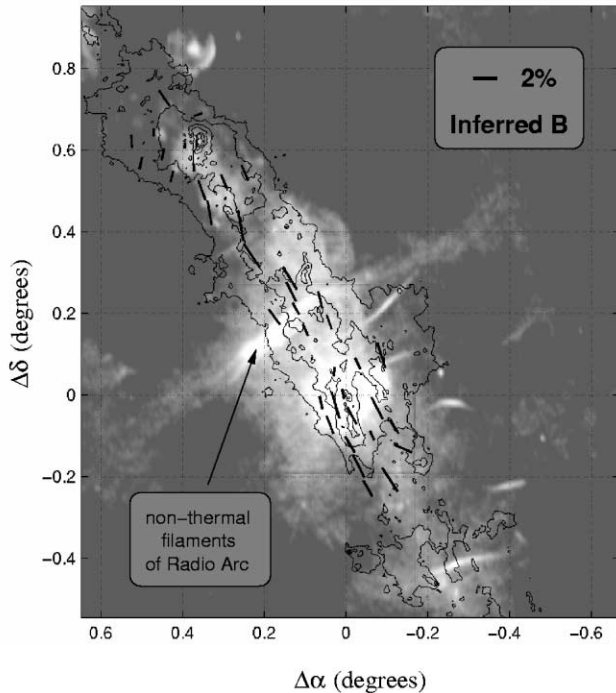


FIG. 2.—The $450\ \mu\text{m}$ polarization measurements (*bars*) shown together with a $90\ \text{cm}$ radio continuum image (*gray scale*; LaRosa et al. 2000) and $850\ \mu\text{m}$ continuum emission (*contours*; Pierce-Price et al. 2000). As in Fig. 1, the orientation of each bar is parallel to the inferred magnetic field direction (i.e., orthogonal to the measured direction of polarization), and its length is proportional to the degree of polarization. The radio continuum image shows about six locations where nonthermal filaments can be seen. These nonthermal filaments trace magnetic fields in hot ionized regions (see § 1). The gray-scale image is logarithmically scaled, and the contours of $850\ \mu\text{m}$ emission are also logarithmic. Coordinate offsets are measured with respect to the position of Sgr A*. The location of the brightest bundle of nonthermal filaments (referred to as the nonthermal filaments of the Radio Arc) is indicated in the figure.

nonthermal filaments, we will use only the more general term, poloidal, to describe the inferred field geometry. It is clear from Figure 2 that the magnetic field in the central few hundred parsecs is neither purely toroidal nor purely poloidal. Rather, there are regions in which toroidal fields dominate as well as regions in which poloidal fields dominate. However, it is not obvious from this figure how these “toroidal-dominant” and “poloidal-dominant” regions are arranged with respect to one another in three-dimensional space.

There does exist a theoretical model for the Galactic center that predicts separate poloidal-dominant and toroidal-dominant regions within the central few hundred parsecs. This is the magnetodynamic model developed by Uchida, Shibata, & Sofue (1985, hereafter USS85) and further refined by Shibata & Uchida (1987). This model was developed in order to explain the “Galactic Center Lobe” (GCL), which is a limb-brightened radio structure with a size of several hundred parsecs extending from the plane of the Galaxy up toward positive Galactic latitudes (Sofue & Handa 1984). In the model of USS85, the GCL represents a gas outflow that is magnetically driven. The model consists of nonsteady axisymmetric magnetohydrodynamic simulations in which the field is assumed to be axial at high Galactic latitudes. Near the Galactic plane, however, the field acquires a toroidal component, as a result of the differential rotation of the dense gas that lies near the plane. The stress of the resultant magnetic twist is what drives the outflow.

One prediction of the USS85 model is that the toroidal component will generally be more dominant for positions nearer

to the Galactic plane (Shibata & Uchida 1987). Yusef-Zadeh & Morris (1988) noted that the nonthermal filaments of the Radio Arc (see Fig. 2) cross the Galactic plane without showing any bending, thus contradicting this prediction. However, SPARO has now revealed extensive toroidal-dominant regions near the Galactic plane, as predicted by USS85.

One way to reconcile these discrepant indicators of field geometry near the Galactic plane is suggested by the clumpy distribution of molecular gas in the Galactic center (see the $850\ \mu\text{m}$ continuum contours in Fig. 2). It may be that at locations in the Galactic plane where the density of molecular gas is relatively lower, the poloidal field can cross this plane with little deformation. Despite the evidence of interaction between the Radio Arc and molecular clouds (Serabyn & Morris 1994; Morris 1998), it could be that the general region of the Galactic plane through which the Radio Arc passes contains relatively less molecular gas as compared with other regions of the Galactic plane. Alternatively, this region may have contained relatively less molecular gas at some time in the past, which has allowed the poloidal field to become locally established. Thus, the model of USS85 may be correct in an overall sense while failing to predict the detailed structure of the field because it ignores the clumpy nature of the gas.

It is possible to probe the line-of-sight component of the magnetic field in any region of the Galactic center that contains thermal gas, provided that this region lies along the line-of-sight to a synchrotron source. This is because polarized radio emission from synchrotron sources suffers Faraday rotation as it passes through thermal gas. We carried out a survey of the literature on Faraday rotation measurements toward Galactic center synchrotron sources, and we discovered a pattern of observed reversals in the sign of the Faraday “rotation measure” (RM) that matches the predictions of the USS85 model. To our knowledge, this pattern in the observations has not yet been fully described, so we discuss it here.

According to the model of USS85, the direction of the line-of-sight field component should exhibit a pattern of reversals that we have illustrated in Figure 3. This figure shows our view of the Galactic center, divided into four quadrants according to the signs of Galactic longitude and latitude. For each quadrant, the direction of the line-of-sight field component is given, together with the corresponding sign of the RM. The pattern shown in Figure 3 is the one that results when the poloidal field points toward positive Galactic latitude. If the poloidal field is taken to point in the negative latitude direction, then all field directions (and RM signs) are reversed. An intuitive understanding of the antisymmetric pattern seen in the figure may be obtained by imagining a system of axial field lines pointing toward Galactic north (“up” in the figure) but suffering a distortion near the Galactic plane, where the upward-directed field lines are being pulled away from the observer on the left side of the figure and toward the observer on the right side.

USS85 compared this predicted pattern with the RM measurements that were available at the time. Specifically, they considered polarimetry of the “northern plume” and “southern plume,” two extended synchrotron-emitting regions that appear to be, respectively, the positive latitude and negative latitude extensions of the nonthermal filaments of the Radio Arc (these filaments are shown in Fig. 2). The two plumes extend out to Galactic latitudes of about $+1^\circ$ and -1° , respectively. USS85 noted that the RM values are predominantly positive for the northern plume, located in the $(+, +)$ quadrant, and predominantly negative for the southern plume, located in the $(+, -)$ quadrant (see also Tsuboi et al. 1986). They remarked that such a sign flip is in accordance with their predictions (see Fig. 3).

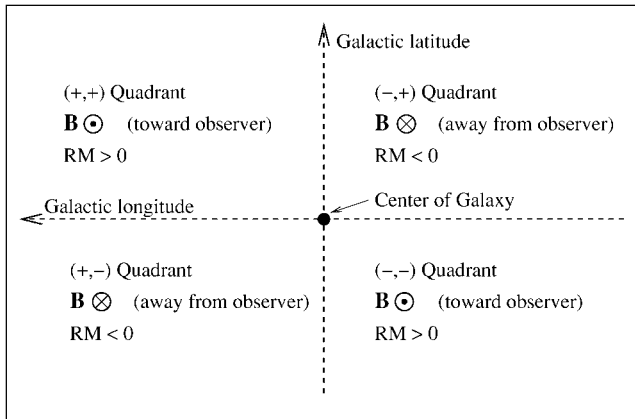


FIG. 3.—Schematic illustration showing how the direction of the line-of-sight magnetic field component should vary, according to the model of USS85. Shown in the figure is our view of the central few hundred parsecs of the Galaxy, divided into four quadrants according to the signs of Galactic longitude and latitude. For each quadrant, the direction of the line-of-sight field component is given, together with the corresponding sign of the Faraday RM. A comparison with observations is given in § 3.

Since the publication of USS85, several papers have reported measurements of Faraday rotation toward individual nonthermal filaments in the Galactic center. In such cases, the Faraday rotation effect is produced in widely dispersed Galactic center gas (Yusef-Zadeh, Wardle, & Parastaran 1997). Here we restrict our discussion to filaments that are found within 1° of Sgr A*.

The RM values observed toward filaments lying in the (+, +) and (+, -) quadrants (Yusef-Zadeh & Morris 1987; Lang et al. 1999) are consistent with the pattern of RM values previously observed in the northern and southern plumes, and thus also with the USS85 model. More interestingly, there are now RM data available for the (-, +) and (-, -) quadrants. Specifically, Yusef-Zadeh et al. (1997) observed negative RM values toward the G359.54+0.18 filament that lies in the (-, +) quadrant, and Gray et al. (1995) found positive RM values for the filament known as the “Snake,” which lies in the (-, -) quadrant. In both cases, the sign of the RM is in accordance with the predicted pattern shown in Figure 3. Considering this pattern of RM reversals together with the SPARO polarization map and the evidence of poloidal fields derived from radio synchrotron maps, we conclude that the available observations do support the general picture given by USS85 for the large-scale magnetic field in the Galactic center.

For technical assistance and valuable suggestions, we thank J. Carlstrom, D. Dowell, M. Dragovan, P. Goldsmith, J. Hanna, A. Harper, R. Hildebrand, R. Hirsch, J. Jaeger, S. Loverde, P. Malhotra, J. Marshall, H. Moseley, S. Moseley, T. O’Hara, R. Pernic, S. Platt, J. Sundwall, and J. Wirth. The SPARO project was funded by the Center for Astrophysical Research in Antarctica (an NSF Science and Technology Center; OPP-8920223), by an NSF CAREER Award to G. N. (OPP-9618319), and by a NASA GSRP award to D. T. C. (NGT5-88). We are grateful to N. E. Kassim, T. N. LaRosa, and D. Pierce-Price for permission to show their data.

REFERENCES

- Dotson, J. L., Novak, G., Renbarger, T., Pernic, D., & Sundwall, J. L. 1998, *Proc. SPIE*, 3357, 543
- Dowell, C. D., Hildebrand, R. H., Schleuning, D. A., Vaillancourt, J. E., Dotson, J. L., Novak, G., Renbarger, T., & Houde, M. 1998, *ApJ*, 504, 588
- Gray, A. D., Nicholls, J., Ekers, R. D., & Cram, L. E. 1995, *ApJ*, 448, 164
- Lane, A. P. 1998, in *ASP Conf. Ser. 141, Astrophysics from Antarctica*, ed. G. Novak & R. H. Landsberg (San Francisco: ASP), 289
- Lang, C. C., Morris, M., & Echevarria, L. 1999, *ApJ*, 526, 727
- LaRosa, T. N., Kassim, N. E., Lazio, T. J. W., & Hyman, S. D. 2000, *AJ*, 119, 207
- Lazarian, A. 2000, in *ASP Conf. Ser. 215, Cosmic Evolution and Galaxy Formation: Structure, Interactions, and Feedback*, *The Third Guillermo Haro Astrophys. Conf.*, ed. J. Franco, L. Terlevich, O. López-Cruz, & I. Aretxaga (San Francisco: ASP), 69
- Morris, M. 1998, in *IAU Symp. 184, The Central Regions of the Galaxy and Galaxies*, ed. Y. Sofue (Dordrecht: Kluwer), 331
- Morris, M., Davidson, J. A., Werner, M., Dotson, J., Figer, D. F., Hildebrand, R. H., Novak, G., & Platt, S. 1992, *ApJ*, 399, L63
- Novak, G., Dotson, J. L., Dowell, C. D., Hildebrand, R. H., Renbarger, T., & Schleuning, D. A. 2000, *ApJ*, 529, 241
- Oka, T., Hasegawa, T., Sato, F., Tsuboi, M., & Miyazaki, A. 1998, *ApJS*, 118, 455
- Peterson, J. B., et al. 2000, *ApJ*, 532, L83
- Pierce-Price, D., et al. 2000, *ApJ*, 545, L121
- Serabyn, E., & Morris, M. 1994, *ApJ*, 424, L91
- Shibata, K., & Uchida, Y. 1987, *PASJ*, 39, 559
- Sofue, Y., & Handa, T. 1984, *Nature*, 310, 568
- Tsuboi, M., Inoue, M., Handa, T., Tabara, H., Kato, T., Sofue, Y., & Kaifu, N. 1986, *AJ*, 92, 818
- Uchida, Y., Shibata, K., & Sofue, Y. 1985, *Nature*, 317, 699 (USS85)
- Vaillancourt, J. E. 2002, *ApJS*, 142, 53
- Yusef-Zadeh, F., & Morris, M. 1987, *ApJ*, 322, 721
- . 1988, *ApJ*, 329, 729
- Yusef-Zadeh, F., Morris, M., & Chance, D. 1984, *Nature*, 310, 557
- Yusef-Zadeh, F., Wardle, M., & Parastaran, P. 1997, *ApJ*, 475, L119